**Title:** Extensive global wetland loss over the last three centuries

**Running head:** Global wetland loss since 1700

**Authors:** Etienne Fluet-Chouinard[1,2,*], Benjamin D. Stocker[3,4,5,6], Zhen Zhang[7], Avni Malhotra[1], Joe R. Melton[8], Benjamin Poulter[9], Jed O. Kaplan[10], Kees Klein Goldewijk[11], Stefan Siebert[12,13], Tatiana Minayeva[14], Gustaf Hugelius[1,15,16], Hans Joosten[17,18], Alexandra Barthelmes[17,18], Catherine Prigent[19,20], Filipe Aires[19,20], Alison M. Hoyt[1], Nick Davidson[21,22], C. Max Finlayson[22,23], Bernhard Lehner[24], Robert B. Jackson[1,25], Peter B. McIntyre[2,26]

**Affiliations:**

[1] Department of Earth System Science, Stanford University, Stanford, California, CA, USA

[2] Center for Limnology, University of Wisconsin-Madison, Madison, WI 53706, USA

[3] Department of Environmental Systems Science, ETH, Universitätsstrasse 2, 8092 Zürich, Switzerland

[4] Swiss Federal Institute for Forest, Snow and Landscape Research WSL, Zürcherstrasse 111, 8903 Birmensdorf, Switzerland

[5] Institute of Geography, University of Bern, Hallerstrasse 12, 3012 Bern, Switzerland

[6] Oeschger Centre for Climate Change Research, University of Bern, Falkenplatz 16, 3012 Bern, Switzerland

[7] Earth System Science Interdisciplinary Center, University of Maryland, College Park, MD 20740, USA

[8] Climate Research Division, Environment and Climate Change Canada, Victoria, BC, Canada

[9] NASA Goddard Space Flight Center, Biospheric Sciences Laboratory, Greenbelt, MD 20771, USA

[10] Department of Earth Sciences, The University of Hong Kong, Hong Kong SAR, China

[11] Faculty of Geosciences, Copernicus Institute of Sustainable Development, Utrecht University, PO Box 80125, 3508 TC Utrecht, The Netherlands

[12] Department of Crop Sciences, Georg-August-Universität Göttingen, Von-Siebold-Str. 8, 37075 Goettingen, Germany

[13] Centre of Biodiversity and Sustainable Land Use (CBL), University of Göttingen, Göttingen, Germany

[14] Care for Ecosystems, Germany

[15] Department of Physical Geography, Stockholm University, Stockholm, Sweden

[16] Bolin Centre for Climate Research, Stockholm University, Stockholm, Sweden

[17] Faculty of Mathematics and Natural Sciences, Peatland Studies and Paleoecology, University of Greifswald, Greifswald, Germany

[18] Greifswald Mire Centre (GMC), Greifswald, Germany.

[19] Sorbonne Université, Observatoire de Paris, Université PSL, CNRS, LERMA, Paris, France

[20] Estellus, Paris, France

[21] Nick Davidson Environmental, Queens House, Ford Street, Wigmore, HR6 9UN, UK.

[22] Institute for Land, Water and Society, Charles Sturt University, Elizabeth Mitchell Drive, PO Box 789, Albury, NSW 2640, Australia

[23] IHE Delft, Institute for Water Education, PO. Box 3015, 2601 DA, Delft, Netherlands

[24] Department of Geography, McGill University, 805 Sherbrooke Street West, Montreal, Canada

[25] Woods Institute for the Environment and Precourt Institute for Energy, Stanford University, Stanford, California, CA

[26] Department of Natural Resources and the Environment, Cornell University, Ithaca, NY, USA

[*] Corresponding author

[*] Current address: Institute for Atmospheric and Climate Science, ETH Zurich, Zurich, Switzerland

**Keywords:** wetland, drainage, land use change, organic soils, historical reconstruction

**Summary Paragraph**

Wetlands have long been drained for human use, thereby strongly affecting greenhouse gas fluxes, flood control, nutrient cycling and biodiversity [1,2]. Yet, the global extent of natural wetland loss remains remarkably uncertain[3]. Here, we reconstruct the spatial distribution and timing of wetland loss through conversion to seven human land uses between 1700 and 2020 by combining national and subnational records of drainage and conversion with land-use maps and simulated wetland extents. We estimate that 3.4 million km$^2$ (C.I. 2.9 - 3.8) of inland wetlands have been lost since 1700, primarily for conversion to croplands. This net loss of 21% (C.I. 16 - 23%) of global wetland area is lower than suggested previously by extrapolations of data disproportionately from high-loss regions. Wetland loss has been concentrated in Europe, the United States, and China, and rapidly expanded during the mid-20$^{th}$ century. Our reconstruction elucidates the timing and land use drivers of global wetland losses, providing an improved historical baseline to guide assessment of wetland loss impact on Earth system processes, conservation planning to protect remaining wetlands, and prioritization of sites for wetland restoration [4].

**Main text**

Throughout most of human history, wetlands have been considered to be 'unproductive land' that is 'ripe for reclamation' for agriculture and urbanization [3]. Draining waterlogged soils has produced some of the most fertile agricultural lands on the planet [5]. Methods like ditch construction and tile drainage date back millennia, while mechanization in the last century has further expedited wetland conversion [6]. Wetland drainage has also been pursued to prevent soil salinization or paludification (i.e., peat formation) [5], to control vector-borne diseases [7], and to extract peat for fuel and soil amendments [8,9]. Together, the deliberate drainage of wetlands plus impacts from climate change, rising sea levels, fires, and groundwater extraction have made wetlands among the most threatened ecosystems in the world [9].

Conserving wetland ecosystems has been recognized formally as an international priority since the *1971 Ramsar Convention*, and was recently affirmed under Indicator *6.6.1* in the United Nations' *Sustainable Development Goals*. These frameworks augment the "*no-net-loss"* policies [10] erected in many nations that shifted away from the subsidy programs encouraging wetland conversion to cropland during much of the 20th century. A central rationale for modern wetland conservation policies is the economic value of the many ecosystem services they support [2,11]. While rates of wetland conversion have declined in most countries, losses continue in some regions, such as Indonesia where tropical peat swamps have been drained for industrial plantations and smallholder agriculture until recently [12,13].

Accurately estimating the extent, distribution and timing of wetland loss is essential to understand their effect on Earth system processes. Wetland losses affect terrestrial water storage [14] , quality and supply [15], evapotranspiration [16], terrestrial-to-ocean carbon export [17], carbon balance [18], emissions of nitrous oxide [19] and methane [20], nutrient removal [21], flood regimes and groundwater recharge [22], and biodiversity [1,23]. Moreover, the environmental legacy of wetland drainage can last for centuries, thereby complicating the accounting of their cumulative impact, particularly for past greenhouse gas emissions arising from historical conversions [24]. Degradation of peatlands, a wetland type characterized by organic soil horizons of >40cm, is particularly impactful due to their major role in soil carbon storage [25,26]. Unlike other major land use transformations, such as deforestation or irrigation, wetland conversion has yet to be reconstructed globally with the temporal and spatial resolution required for Earth system simulations [27].

High estimates of wetland loss have been reported in the literature for decades [1,28,29], for example that '*50% of the world's wetlands have been lost since 1900*' [1,30]. More recent estimates based on regional extrapolations [3,31] and geospatial overlay approaches [16,32] have ranged between 28% to 87% net losses since 1700. These disparities undermine the credibility of broad comparisons to loss rates of other ecosystem

types, for example forests [28,29]. A rigorous estimation of wetland loss has been hindered by the paucity of historical data, requiring the unifying of data and modeling approaches.

Here, we use a two-step approach to estimate the conversion of wetlands into seven classes of human land use between 1700 and 2020 (Figure S1; see Methods). Our analysis focuses on inland wetlands, which we define as any area inundated or waterlogged for at least one continuous month during the period of record, regardless of surface vegetation, but excludes permanently inundated areas (river channels and lakes), coastal intertidal zones and near-shore marine wetlands. First, we compiled a database of 3320 national and subnational drainage and land-use records, on area converted and peat mass extracted, from 154 countries and across four land uses (*cropland, forestry, peat extraction, and wetland cultivation*; Figure S2, S3 and S4). We interpolated the country-level drainage records into continuous time series, then spatially distributed the drained area in proportion to the joint probability of each of the four land uses and the potential wetland cover fractions in each 0.5° grid cell globally. Second, we supplemented the national statistics by modeling three additional land-use classes that also cause wetland conversion (*irrigated rice, pasture, and urban areas*), which were calibrated to maximize agreement with 121 geolocated independent regional estimates of percentage wetland area change. This approach unifies the main available information sources on wetland loss to produce a comprehensive, data-driven estimate at the global scale.

### *Global drivers of wetland loss*

We estimate that the global area of natural wetlands has declined by 3.4 million $km^2$ (C.I.: 2.9 - 3.8 $Mkm^2$) since 1700 (Figure 1A, B and C). This estimate corresponds to a loss of 21% (C.I. 16 - 23%) of the 15.8 $Mkm^2$ (C.I. 13.6 - 17.5 $Mkm^2$) of wetlands estimated to exist in 1700 (Figure 1D). We label the total area affected by conversion to these seven land uses as '*wetland loss*,' though we recognize that they vary in severity of impacts, ranging along a gradient from full drainage and replacement of natural wetland (e.g., upland cropland, forestry, urban areas, pasture), to drainage and soil degradation (e.g., peat extraction), to conversion to artificial wetlands with controlled water levels (e.g., irrigated rice and wetland cultivation).

Wetland drainage for upland croplands was the most common cause of loss of natural wetlands (2.0 $Mkm^2$; 61.7% of total loss), followed by conversion to flooded rice (18.2%), urban areas (8.0%), forestry (4.7%), wetland cultivation (4.3%), pasture (2.0%) and peat extraction (0.9%; Figure 1E). Despite its limited global importance, forestry was the dominant driver of wetland loss in Sweden, Finland and Estonia, accounting for >45% of total losses in these countries (Figure 1F). We estimate that 792 million tonnes of dry peat have been extracted since 1700 for fuel or fertilizer, leading to the degradation of 0.026 $Mkm^2$ of peatlands. Peatland degradation was concentrated primarily in Ireland, Northern Europe and Western Russia. Conversion to flooded rice or other wetland cultivation systems is another regionally important driver of loss, particularly in Asia and Sub-Saharan Africa where they account for ~40% of all losses[33].

The highest global rates of wetland area loss (0.46 $Mkm^2\ yr^{-1}$ or 2.2% $year^{-1}$) occured in the 1950s when government programs subsidized drainage for agriculture and forestry across North America, Europe and China [34] (Figures 1A and S7). However, the scarcity of drainage records before 1850 could lead to an underestimation of losses in countries with known early drainage or peat extraction. Thus, our estimates of both long-term trends and cumulative losses may be underestimated if early wetland conversions were not recorded in later surveys.

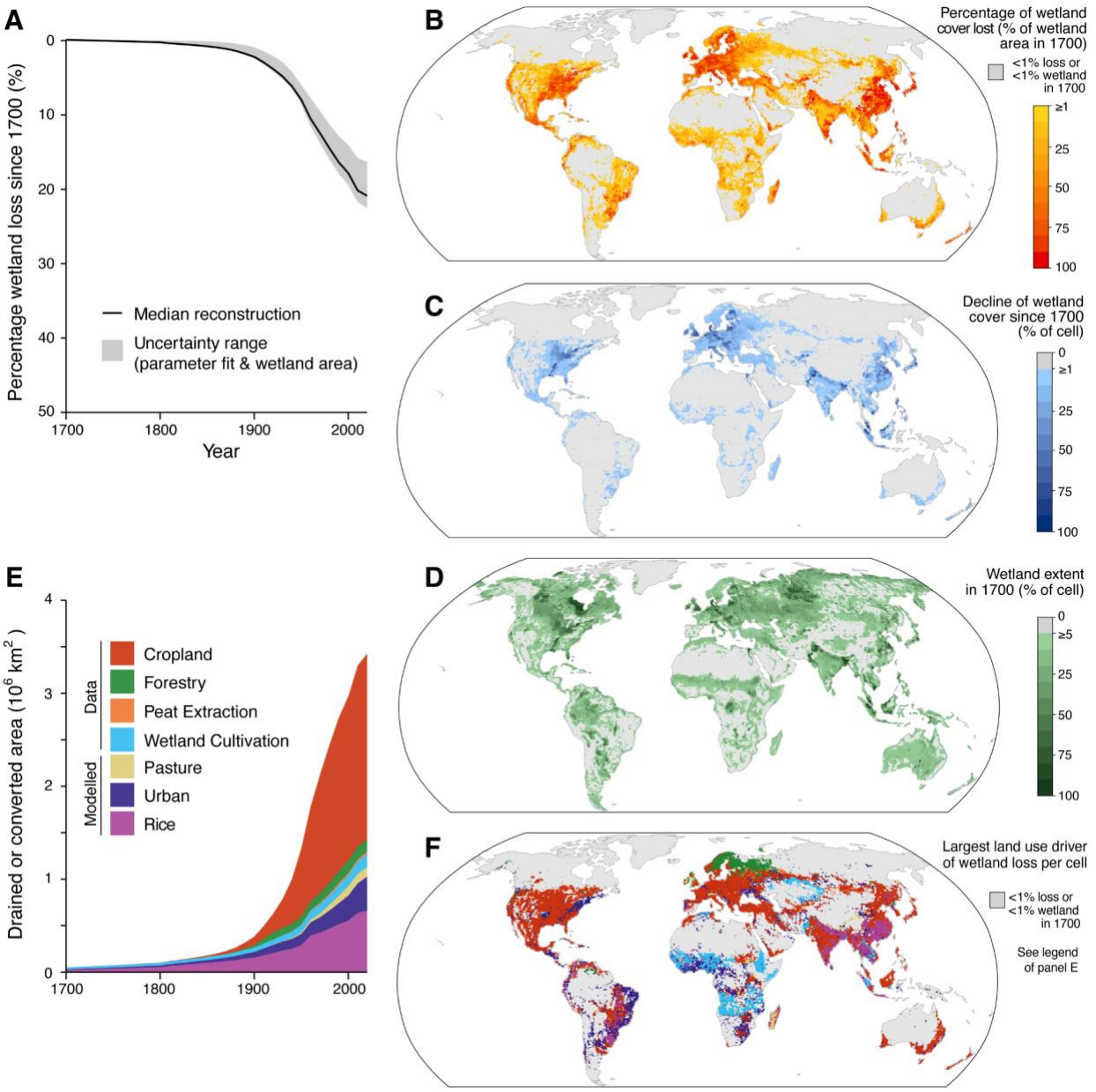


***Figure 1: A)*** *Cumulative loss of global wetland area from 1700 to 2020; estimated global loss rates were modest through 1900 but accelerated afterwards. The uncertainty band (grey) is derived from the ensemble of permutations of parameters and wetland maps used to calculate wetland loss (See Methods).* ***(B)*** *Map of cumulative percent wetland loss as a fraction of wetland cover in 1700.* ***(C)*** *Map of wetland extent decline calculated as difference in wetland cover between 1700 and 2020.* ***(D)*** *Map of natural wetland extent in 1700.* ***(E)*** *Cumulative drivers of wetland loss by land use class through 2020; cropland and rice cultivation are the primary uses of converted wetlands worldwide.* ***F)*** *Map of the dominant land use for converted wetlands. See Figure S5 for individual land use maps.*

***Regional hotspots of loss***

Regional hotspots, where >50% of wetlands were lost between 1700 and 2020, are found in the United States, Europe, Central Asia, India, China, Japan and Southeast Asia (Figure 1B & 2A). Although we find no justification for the generalization that '*more than half of the world's wetlands have been lost*' [1], several nations do exceed that threshold (Table S1). Just five countries account for >40% of all global wetland losses: USA (15.6% of total), China (12.6%), India (6.5%), Russia (4.5%), and Indonesia (4.1%).

We estimate that 0.51 $Mkm^2$ (11%) of peatlands have been lost when accounting for all seven land use classes. This figure is similar to the 0.5 M $km^2$ peatland loss estimated previously by land use overlays [35]. Among peatland-rich regions, Northern European peatlands have undergone the earliest and highest losses since 1700, followed by a recent increase of peatland drainage in Indonesia and Malaysia for oil palm cultivation (Figure 2B). Peatland losses in Indonesia and Malaysia are underestimated by our reconstruction, even if guided by regional data indicating high peatland loss [13] because our reconstruction method conflates all wetland types when allocating drainage to both peatland and non-peatland areas. In contrast, the vast northern peatlands of Siberia and Canada have been largely spared from human conversion to date, but our estimates exclude regionally significant mining and oil extraction [36]. Draining peatlands merits special attention due to release of soil organic carbon accumulated over millennia under low redox conditions as greenhouse gases to the atmosphere [18,25].

Among the world's major river basins, most wetland losses occurred in populated temperate watersheds such as the Danube, Indus, Yangtze, and Mississippi rivers (Figure 2C). Substantial wetland loss across river basins can lead to increased flooding [37] and degraded water quality [15,38]. These impacts are also caused by the loss of geographically isolated wetlands, which rarely benefit from the same protection as those connected to navigable waters [39]. To date, some tropical river basins such as the Amazon and Congo have retained most of their riparian wetlands, thereby protecting the role of their lateral river-floodplain connectivity for ecosystem productivity and carbon export [40].

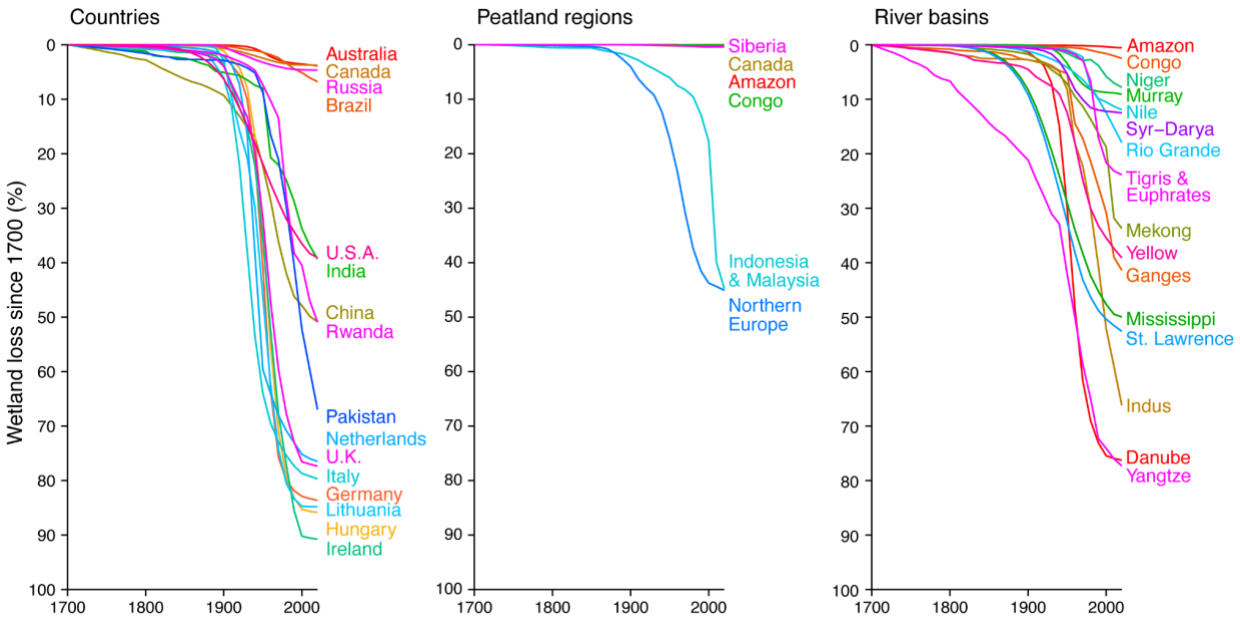


***Figure 2:*** *Percentage of wetland loss since the 1700 baseline within (A) selected countries, (B) peatland-dense regions (see peatland regions in Figure S7), and (C) major river basins. See section 'Regional summary of wetland loss' in Methods for details.*

### *Calibration to regional data*

We reconciled drainage statistics and wetland loss data in many regions, ensuring that our global approach aligns with the best available regional estimates of wetland loss. Specifically, we modeled losses to three key classes of land use (*irrigated rice*, *pastures and urban areas*) based on 121 geolocated regional estimates of percentage wetland conversion (Figure 3A). These regional estimates derived from soil maps and local records are the closest available proxies to direct measurements of historic wetland area and change (see Methods). Following calibration and fitting, our reconstruction achieved reasonable agreement with these independent estimates (Figure 3B, $R^2$ ensemble range = 0.62-0.74), and successfully identified most known hotspots of wetland loss.

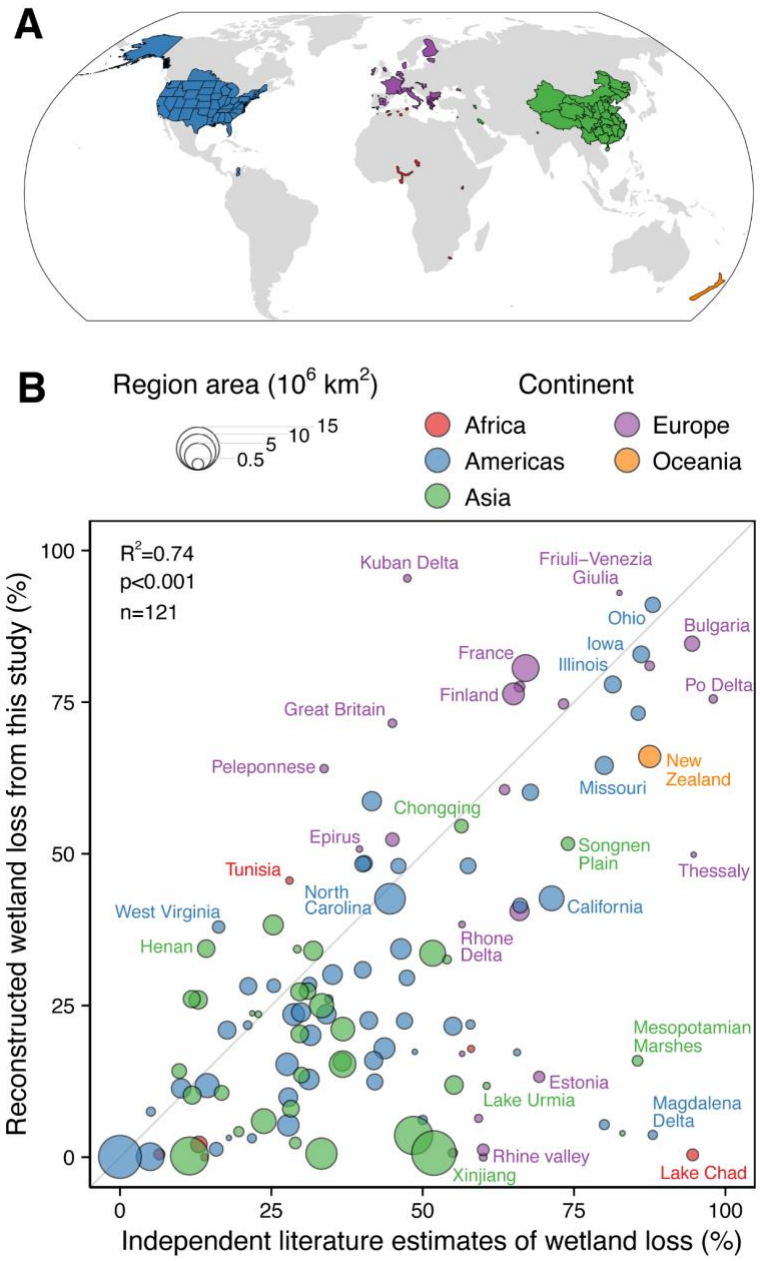


***Figure 3:*** *A) Areas covered by 121 regional wetland loss estimates (see legend in panel B for colors by continent) compiled from independent databases. (B) Comparing our reconstructed wetland losses (y-axis) against reported regional losses (x-axis) indicates high overall agreement, particularly in regional hotspots of conversion. The region area (circle size) was used as a weighting term for calibrating our reconstruction to the regional estimates, showing that the most discrepant regions cover smaller areas.*

### *Discrepancies with global loss estimates*

The patchiness of available historical data on wetland drainage and our restrained imputation over data gaps likely led our loss estimates to be conservative, as illustrated by the negative bias (-14 to -23%; Figure 3B) indicating modest underestimation by our reconstruction relative to regional data. Yet, the magnitude of this mismatch is far less than the disparity between our global wetland loss estimate and prior findings from

meta-analyses (Figure 4). Published extrapolations of regional estimates of annual wetland change (% year$^{-1}$) data put global losses as high as 87% since 1700 [3] and 35% since 1970 [31]. These extrapolations are based on historic records and land use and soil maps which, even if they were locally accurate, are unlikely to be representative of wetland heterogeneity across the globe [3,31]. Indeed, comparing the statistical distribution of regional loss rates to that of all grid cells in our reconstruction suggests a strong bias of regional studies toward high-loss areas (two-tailed Kolmogorov-Smirnov (KS) test; D=0.48-0.61; p<0.0001; Figure S8), likely causing overestimated global wetland losses. Our exclusion of marine wetlands (e.g., mangroves), which are included in other global estimates (Figure 4), is unlikely to explain the overall disparity because marine wetlands are modest in aggregate area relative to inland wetlands [3].

The geography of wetland losses indicated by our global reconstruction also contrasts with previous spatial analyses. Geospatial overlays of cropland and urban land use maps upon an idealized potential wetland cover suggest cumulative conversion of 28-33% [16,25,32], which is roughly comparable to our reconstruction (Figure 4). However, some geospatial-overlay estimates [32] differ sharply in geographic distribution from our reconstruction, particularly in suggesting greater losses in South America (Table S2). The large uncertainty of their spatial patterns reflect disagreement of underlying land use and potential wetland extents [41] as well as differing interpretations of their spatial overlap [18].

Although our reconstruction likely underestimates wetland loss since 1700 in some regions, the global cumulative losses are unlikely to be severely underestimated for several reasons. First, our reconstruction captures the largest centers of drainage across North America, Europe and Asia, and the regions with data gaps are insufficient to substantially increase the estimated global loss. Second, we likely overestimated loss in arid regions where drainage (e.g., Pakistan) is installed to prevent soil salinization from irrigation but is interpreted as wetland loss by our method [42]. Third, among our ensemble of reconstructions using different wetland maps, the global estimates all converged on similar percentage losses because the higher wetland area from some maps was offset by higher wetland area losses (Figure S9).

Resolving the recent declines in wetland area is essential for evaluating progress toward the *Sustainable Development Goal (SDG) 6.6.1*: *Change in the extent of water-related ecosystems over time*, and our reconstruction fills an important knowledge gap. Indeed, SDG 6.6.1 benchmarks wetland loss against a 1970 baseline, and the gap between our reconstruction and extrapolated rates of loss is magnified during this recent period. However, comparing our long-term reconstruction and regional extrapolations since 1970 [31] suggests that even increased density of the monitoring network has not overcome biases arising from reliance on high-loss sites and a shifted baseline (two-tailed KS test; D=0.31-0.46; p-value<0.0001; Figure S8). In the future, it will be important to expand monitoring in ways that diminish biases in the network of sites used to represent global dynamics of wetland losses.

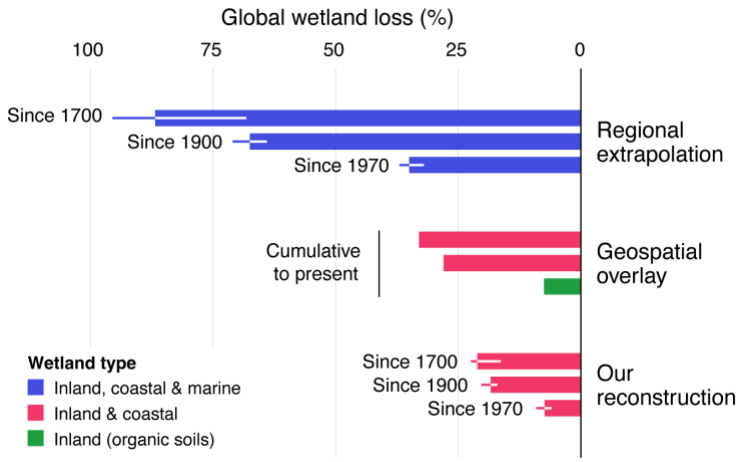


***Figure 4:*** *Comparison of global wetland loss estimates from the literature and this study diverge markedly, with our reconstruction suggesting losses are lower than most previous estimates (each bar is an individual estimate). The highest losses are estimated by meta-analyses extrapolating regional records of percentage loss. Geospatial overlays generate similar percentage loss estimates to our reconstruction, but some diverge in their starting baseline and geographic distribution of loss. Sources also vary in the drivers included (meta-analysis includes mining, overgrazing, etc.; geospatial overlays include only cropland and urban), and have their own respective wetland type definitions (e.g. coastal). See Table S3 for sources.*

### *Conclusions*

Our reconstruction of three centuries of wetland conversion draws upon both drainage statistics and regional loss estimates to produce a temporally-explicit trajectory of global wetland extent. These results reveal that most previous studies overestimated global wetland conversion by relying on data concentrated in high loss regions. However, our findings should not lessen the urgency to protect and restore wetland ecosystems, particularly in regions with ongoing rapid drainage as well as remnants located in high-loss regions.

Our maps of wetland extent, conversion rates, and land use drivers enable numerous applications. This information provides a baseline for conservation targets and prioritizing protection of wetland types and dependent species. In a restoration context, understanding land use histories helps choose sites for interventions such as rewetting to reduce radiative forcing or enhance nutrient removal [4]. For Earth system modeling, the extent of wetland conversion is essential to quantify the full anthropogenic impact on carbon and water budgets [17,20]. As the world's wetlands face further pressures in the coming decades, extending our reconstruction with continuous monitoring of wetland cover via remote sensing [43], national reporting and networks of sites is urgently needed.

## References


1. Zedler, J. B. & Kercher, S. Wetland Resources: Status, Trends, Ecosystem Services, and Restorability. *Annual Review of Environment and Resources* vol. 30 39–74 (2005).
2. Finlayson, C. M. *et al. Millennium Ecosystem Assessment: Ecosystems and human well-being: Wetlands and Water Synthesis*. (2005).
3. Davidson, N. C. How much wetland has the world lost? Long-term and recent trends in global wetland area. *Mar. Freshwater Res.* **65**, 934 (2014).
4. Günther, A. *et al.* Prompt rewetting of drained peatlands reduces climate warming despite methane emissions. *Nat. Commun.* **11**, 1644 (2020).
5. Schultz, B., Thatte, C. D. & Labhsetwar, V. K. Irrigation and drainage. Main contributors to global food production. *Irrigation and Drainage* vol. 54 263–278 (2005).
6. Valipour, M. *et al.* The Evolution of Agricultural Drainage from the Earliest Times to the Present. *Sustainability* vol. 12 416 (2020).
7. Holden, J., Chapman, P. J. & Labadz, J. C. Artificial drainage of peatlands: hydrological and hydrochemical process and wetland restoration. *Progress in Physical Geography: Earth and Environment* vol. 28 95–123 (2004).
8. Joosten, H. & Clarke, D. Wise use of mires and peatlands. *International Mire Conservation Group and International Peat Society* **304**, (2002).
9. van Asselen, S., Verburg, P. H., Vermaat, J. E. & Janse, J. H. Drivers of wetland conversion: a global meta-analysis. *PLoS One* **8**, e81292 (2013).
10. Maron, M. *et al.* The many meanings of no net loss in environmental policy. *Nature Sustainability* vol. 1 19–27 (2018).
11. Costanza, R. *et al.* The value of the world's ecosystem services and natural capital. *Nature* vol. 387 253–260 (1997).
12. Page, S. E. & Hooijer, A. In the line of fire: the peatlands of Southeast Asia. *Philos. Trans. R. Soc. Lond. B Biol. Sci.* **371**, (2016).
13. Miettinen, J., Shi, C. & Liew, S. C. Land cover distribution in the peatlands of Peninsular Malaysia, Sumatra and Borneo in 2015 with changes since 1990. *Global Ecology and Conservation* **6**, 67–78 (2016).
14. Wada, Y. *et al.* Recent Changes in Land Water Storage and its Contribution to Sea Level Variations. *Surv. Geophys.* **38**, 131–152 (2017).
15. Xu, J., Morris, P. J., Liu, J. & Holden, J. Hotspots of peatland-derived potable water use identified by global analysis. *Nature Sustainability* vol. 1 246–253 (2018).
16. Sterling, S. M., Ducharne, A. & Polcher, J. The impact of global land-cover change on the terrestrial water cycle. *Nature Climate Change* vol. 3 385–390 (2013).
17. Abril, G. & Borges, A. V. Ideas and perspectives: Carbon leaks from flooded land: do we need to replumb the inland water active pipe? *Biogeosciences* **16**, 769 (2019).
18. Qiu, C. *et al.* Large historical carbon emissions from cultivated northern peatlands. *Science Advances* vol. 7 eabf1332 (2021).
19. Bahram, M. *et al.* Structure and function of the soil microbiome underlying N2O emissions from global wetlands. *Nat. Commun.* **13**, 1430 (2022).
20. Paudel, R., Mahowald, N. M., Hess, P. G. M., Meng, L. & Riley, W. J. Attribution of changes in global wetland methane emissions from pre-industrial to present using CLM4.5-BGC. *Environ. Res. Lett.* **11**, 034020 (2016).
21. Cheng, F. Y., Van Meter, K. J., Byrnes, D. K. & Basu, N. B. Maximizing US nitrate removal through wetland protection and restoration. *Nature* **588**, 625–630 (2020).

22. Bullock, A. & Acreman, M. The role of wetlands in the hydrological cycle. *Hydrol. Earth Syst. Sci.* **7**, 358–389 (2003).

23. Castellano, M. J., Archontoulis, S. V., Helmers, M. J., Poffenbarger, H. J. & Six, J. Sustainable intensification of agricultural drainage. *Nat Sustain* **2**, 914–921 (2019).

24. IPCC. *2013 Supplement to the 2006 IPCC Guidelines for National Greenhouse Gas Inventories: Wetlands: Methodological Guidance on Lands with Wet and Drained Soils, and Constructed Wetlands for Wastewater Treatment*. (2013).

25. Tubiello, F., Biancalani, R., Salvatore, M., Rossi, S. & Conchedda, G. A Worldwide Assessment of Greenhouse Gas Emissions from Drained Organic Soils. *Sustainability* vol. 8 371 (2016).

26. Hugelius, G. *et al.* Large stocks of peatland carbon and nitrogen are vulnerable to permafrost thaw. *Proc. Natl. Acad. Sci. U. S. A.* **117**, 20438–20446 (2020).

27. Pongratz, J. *et al.* Models meet data: Challenges and opportunities in implementing land management in Earth system models. *Glob. Chang. Biol.* **24**, 1470–1487 (2018).

28. Intergovernmental Science-Policy Platform on Biodiversity and Ecosystem Services (IPBES), (2018). *Land degradation assessment. (2018)*.

29. Ramsar Convention Secretariat, Ramsar Convention on Wetlands. (2018). *Global Wetland Outlook: State of the World's Wetlands and their Services to People*.

30. Winkler, M. G. & DeWitt, C. B. Environmental Impacts of Peat Mining in the United States: Documentation for Wetland Conservation. *Environ. Conserv.* **12**, 317–330 (1985).

31. Darrah, S. E. *et al.* Improvements to the Wetland Extent Trends (WET) index as a tool for monitoring natural and human-made wetlands. *Ecol. Indic.* **99**, 294–298 (2019).

32. Hu, S., Niu, Z., Chen, Y., Li, L. & Zhang, H. Global wetlands: Potential distribution, wetland loss, and status. *Sci. Total Environ.* **586**, 319–327 (2017).

33. Verhoeven, J. T. A. & Setter, T. L. Agricultural use of wetlands: opportunities and limitations. *Ann. Bot.* **105**, 155–163 (2010).

34. Pavelis, G. A. *Farm Drainage in the United States: History, Status, and Prospects*. (1987).

35. Leifeld, J. & Menichetti, L. The underappreciated potential of peatlands in global climate change mitigation strategies. *Nat. Commun.* **9**, 1071 (2018).

36. Rooney, R. C., Bayley, S. E. & Schindler, D. W. Oil sands mining and reclamation cause massive loss of peatland and stored carbon. *Proc. Natl. Acad. Sci. U. S. A.* **109**, 4933–4937 (2012).

37. Acreman, M. & Holden, J. How Wetlands Affect Floods. *Wetlands* vol. 33 773–786 (2013).

38. Creed, I. F. *et al.* Enhancing protection for vulnerable waters. *Nat. Geosci.* **10**, 809–815 (2017).

39. Cohen, M. J. *et al.* Do geographically isolated wetlands influence landscape functions? *Proc. Natl. Acad. Sci. U. S. A.* **113**, 1978–1986 (2016).

40. Borges, A. V. *et al.* Divergent biophysical controls of aquatic CO2 and CH4 in the World's two largest rivers. *Sci. Rep.* **5**, 15614 (2015).

41. Melton, J. R. *et al.* Present state of global wetland extent and wetland methane modelling: conclusions from a model inter-comparison project (WETCHIMP). *Biogeosciences* **10**, 753–788 (2013).

42. Ritzema, H. P. Drain for Gain: Managing salinity in irrigated lands—A review. *Agricultural Water Management* vol. 176 18–28 (2016).

43. Gallant, A. The Challenges of Remote Monitoring of Wetlands. *Remote Sensing* vol. 7 10938–10950 (2015).

## Methods

### *Methodological Overview*

We used five primary data sources to produce a gridded reconstruction of wetland loss: 1) national and subnational statistics reporting wetland area drained or converted, 2) regional data on percentage wetland loss, 3) present-day wetland maps, 4) simulated wetland maps, and 5) reconstructed land use maps. Our methodology combines all input data to produce a globally gridded reconstruction of wetland drainage, conversion and degradation over 1700-2020.

Our approach to reconstructing global wetland loss consists of four steps (see Figure S1 for a schematic summarizing methods). National statistics for four land use drivers (*cropland, forestry, peat extraction, and wetland cultivation*) were first interpolated into continuous time series (at 10 year intervals; the timestep of the analysis). Second, potential wetland area was generated from maps of present-day wetlands and simulations of idealized wetland cover. The national drainage time series were then mapped on a 0.5° grid based on the geographic distribution of land use and potential wetland. This mapping was conducted simultaneously with three additional land uses (*irrigated rice, pasture, urban areas*) whose land use conversion was modeled based on potential wetland and land use maps. Fourth, once land use drainage and conversion was mapped, the resulting wetland loss was compared against 121 independent regional estimates of percentage wetland loss. The last two steps of mapping and comparison were repeated through an optimization process until optimal parameter values maximizing agreement were found.

Our reconstruction model focuses on long-term wetland losses and therefore does not represent wetland gains resulting from drainage disrepair, land use abandonment or wetland restoration. We use 'wetland loss' as a catch-all term for "drainage, conversion, degradation or regulation", and our global figures on wetland loss should not be understood to cause a similar decline of ecosystem function across the world.

### *Wetland definition*

We define the inland and coastal wetlands included in our analysis based on a methodological rather than an *a priori* definition or typology. Our operational wetland definition is inherited from wetland maps we used which represent wetlands on land and above the maximum tide-line. These maps (described below) represent areas that are inundated or waterlogged, vegetated or not (e.g., forested swamps, bare floodplains), from which we removed open water ecosystems (e.g., rivers, reservoirs and lakes), rice paddies, and the annual maximum water extent along coastlines. As a result, intertidal and near-shore marine wetlands (e.g., unvegetated tidal flats, salt marshes, mangroves, seagrasses) are excluded, but coastal wetlands above the tideline remain (e.g., deltas). Wetlands are land inundated or saturated by water intermittently, periodically or seasonally, because we used a minimum period of inundation or saturation of 1 month over the respective observation periods (13-15 years) to be considered a wetland. This maximalist definition is used to balance the known gaps in wetland maps for small wetlands and below dense canopy.

### *Input data*

*National drained area statistics:* Data on area artificially drained or cultivated in wetlands, as well as the volume of peat extracted have been collected by state agencies for decades as part of agricultural or economic surveys. We compiled 3320 national and subnational records of the area drained or wetlands converted to different land uses (Figure S2). We classified national scale data (n=1949) into four land uses: cropland (n=396, 20.3% of national data count), forestry (n=58, 3.0%), peat extraction (n=1291; 66.2%) and wetland cultivation (n=204, 10.5%; Figure S3). The subnational data (n=1371) were similarly organized into four land uses, but with different relative shares of land use drivers: cropland (n=1020, 74.4% of subnational total), forestry (n=57, 4.2%), peat extraction (n=284; 20.7%), and wetland cultivation (n=10, 0.7%; Figure S4). The database covers 154 countries and is concentrated in the post-1950 period (average and standard deviation; national: 1977 ±32; subnational: 1981 ±53; Figure S10 and S11). Documentation

of wetland conversion prior to 1900 is sparse. We chose the baseline of 1700 to capture the time period before national drainage statistics were first recorded, allowing us to assume that the entire drained wetland area included in national and subnational statistics was drained after 1700. We acknowledge that drainage is known to have emerged prior to 1700 in several places, for example for agriculture in Egypt, Mesopotamia, India, China [6] and for peat extraction in the Netherlands [44]. That this early drainage affects the baseline of our relative wetland loss quantification, but not our absolute area estimates. Refining estimates of early losses and pre-1700 wetland extent will likely require new paleo-ecological data such as pollen and sediment records [45].

Cropland drainage statistics were compiled from existing databases and publications, mainly from Pavelis (1987) [34], Feick et al. (2005) [46], the International Commission on Irrigation and Drainage (ICID) [47], and the Food and Agriculture Organization (FAO) [48]. We also compiled data on the start year of subsidy programs for the formation of drainage districts in the United States to constrain the temporal model of drainage. We assumed drainage was negligible before the start of subsidies because, nearly everywhere, data on drained areas are only available decades after the recorded initiation of drainage projects. This assumption is adequate for regions where data collection coincided with state-sponsored reclamation projects (e.g., states affected by the Swamp and Overflowed Lands Act of 1850 [34,49]). We used a ranking of data sources from manual interpretation to resolve conflicting data for the same countries and time periods which may originate from differences in drainage or land use definitions, generally selecting larger areas from more encompassing definitions.

For wetland cultivation, we compiled data from the Food and Agriculture Organization's (FAO) FAOSTAT [48] on the area cultivated under the following practices: lowland cultivation, flood recession agriculture, and spate irrigation. Wetland cultivation practices were separated from other drainage types because they maintain wet or inundated conditions during part of the year, and thus do not functionally replace wetland ecosystems. Yet, we consider this transition to management by humans as a loss of the natural wetland ecosystem. Despite our attempt to treat land use classes as mutually exclusive in our methodology, some double-counting is possible between cropland, irrigated rice and wetland cultivation in regions where data definitions overlap and are challenging to resolve.

For peat extraction, we collected data on dry peat mass extracted annually (tonnes per year; excluding briquettes and other processed fuels) as well as on the area of peatland drained for extraction. Peat mass and area were combined in a cumulative time series (see section below: Drained area time series hindcasting). The rise and decline in annual peat extraction rates during the 20th century could be captured for certain countries; whereas for other countries the compiled data only represented their decline, although earlier peat extraction industries are documented (e.g., Netherlands[44], Ireland[50]), leading to a likely underestimation of the oldest peat drainage.

Despite being the most common method of wetland reclamation, installation of surface or subsurface drainage can occur also outside of wetlands. Artificial drainage can be installed in upland areas to prevent salinization, paludification, or to improve growing conditions [42,51]. National statistics rarely specify the objective of drainage, preventing us from distinguishing between drainage leading to wetland loss or not. However, in temperate, humid and semi-humid climatic zones, where most of drainage records originate, drainage is primarily designed for reclamation of wet and waterlogged lands [51].

*Regional data on wetland fraction lost:* Regional estimates of wetland area or their fraction lost have been reported across the world from a variety of approaches: land and soil surveys, land use conversion records, historic hydric soils maps, and remote sensing. Such data provide the best available benchmark and calibration target for our reconstruction. We compiled estimates from four data sources: [3,31,52,53]. Most data originate from country-wide assessments for the USA (1780-1980[53]) and China (1978-2008[52]). We then filtered these data using four screening criteria to keep only records that: i) include inland wetlands, and

not exclusively coastal or man-made wetlands, ii) cover an area >10,000 km$^2$, 3) span a time period ≥30 years, and iv) provide both a start and end year. Application of these criteria ensured the regions would provide a comparison at scales detectable by the reconstruction. We then geographically delineated 121 non-overlapping regions (Figure 3A) for which available data met these criteria and consulted the original sources for maps or descriptions wherever possible. Some regional estimates are likely geographic extrapolations from smaller local estimates within those regions. The resulting 121 regional estimates collectively cover 16% of the world's land mass, occupying 190,000 km$^2$ on average (s.d. 280,000 km$^2$) and spanning an average of 125 years (s.d.: 87.6).

*Present-day wetland cover:* Present-day wetland area distributions were taken from three sources: WAD2M (13.8 Mkm$^2$) [54] and GIEMS v2.0 [55] (12.5 Mkm$^2$), produced from multi-sensor remote sensing, and GLWD (10.9 Mkm$^2$), compiled from a selection of maps and charts [56] , which were provided in original resolutions of 0.25°, 0.25°, and 0.0083° (30 arc-second), respectively. Several pre-processing steps were required to produce three comparable static wetland maps. First, we calculated the maximum inundated area fraction for each grid cell from the WAD2M and GIEMSv2 monthly time series. Second, we processed GIEMSv2 following the method previously used to generate WAD2M[54] to only retain vegetated wetlands: subtract the area fraction of open water bodies [57], ocean water cover [58] and irrigated rice area[59], within 0.5° grid cells, but retain a minimum wetland fraction from wetland maps that represent saturated soils rather than inundation [60,61]. The exclusion of ocean water cover at high tide leads our reconstruction to include inland and coastal wetland but exclude off-shore marine wetlands. Third, GLWD classes 4 to 12 were selected to only include vegetated wetland classes (excluding rivers, lakes and reservoirs) and aggregated to 0.5° grid cells. As a result, the three wetland maps represent the maximum extent of seasonally inundated or water-saturated land areas, excluding open water bodies, rice paddies and off-shore marine wetlands. Our three wetland maps diverge in the extent of global wetland area by 2.9 Mkm$^2$ (10.9 to 13.8 km$^2$; 23% of the average) and in their geographic distribution (Figure S12). The differences in time-period covered, 2000-2018 for WAD2M, 1992-2015 for GIEMSv2 and 1970s-1990s for GLWD, is unlikely to be a major source of disagreement in the global wetland area.

*Simulated wetland cover:* We used the cell-wise maximum simulated wetland area fraction from grids of simulated monthly time series, to inform the spatial mapping of drainage statistics and to estimate the extent of losses from the three modeled land uses (*irrigated rice, pasture, and urban areas*). We used four simulated wetland cover datasets from four land surface models: ORCHIDEE, SDGVM and DLEM, compiled for a multi-model intercomparison project [41], and from LPJ-wsl [62] (Figure S13). Each model dynamically simulates wetland extent as the fraction of the inundated area in each grid cell, using sub-grid scale topography information and following a TOPMODEL approach[63]. The water table is simulated in response to soil type, runoff and the local water balance. These models do not simulate surface hydrodynamics, and hence likely underestimate the area of riverine floodplains and coastal wetlands. Importantly, simulations exclude the direct impact of human land use as a driver of wetland loss, and thus represent areas where wetlands should naturally form. The simulated wetland area of all models represents the period 1993-2004 and was generated from transient model simulations forced over 1932-2009 [64]. We took the grid-cell maximum over 1993-2004 for each model and used the four resulting static simulated wetland cover for 1700-2020, thereby ignoring any climate-driven change in wetland area and distribution since 1700. Among models, the range of simulated global natural wetland extents is wide (12.0 - 64.6 Mkm$^2$) and much larger than the fluctuations over time within individual models. This led us to use these data only to inform the spatial distribution of wetland conversion rather than its overall magnitude. All maps were resampled to a grid cell resolution of 0.5° prior to calculations.

*Reconstructed land use maps:* We used gridded historical land use estimates to inform the spatial allocation of drainage data, as well as help determine the extent of wetland losses from the three modeled land uses (*irrigated rice, pasture, and urban areas*). We used the land use maps from HYDE 3.2 [65] to represent

cropland, pasture, irrigated rice, and urban areas since 1700. The area occupied by each land use is estimated in HYDE3.2 from population hindcasts and assumed per capita land-use requirements [66]. Cropland area (upland seasonal and perennial crops) was used to map both conversion to croplands as well as for wetland cultivation (their respective area from national records was mapped sequentially), while the other wetland loss drivers were matched one-to-one with their respective land use. Data on the forest area (primary and secondary forests) affected by wood extraction were taken from LUH2 [67]. To map peat extraction, we converted a global polygon-based peatland map [68] to a 0.5° grid. We used a single set of land use maps rather than an ensemble because our approach required us to separate specific land use classes (e.g., irrigated rice, forestry) that are only available from different sources. Moreover, historical land use maps do not diverge significantly over the 1800-2000 period when most of the drainage occurs.

***Reconstruction methodology***

*Drained area time series hindcasting:* We reconstructed time series of the drained area in cropland and forestry by fitting sigmoidal functions using a non-linear optimizer with multiple starting points [69]. A separate sigmoid function was fitted to the national data from 18 countries and land use type combinations (Figure S14) with sufficient number of data points (≥4) where robust fitting parameters could be achieved (Eufron's pseudo $R^2$ median: 0.90, range: 0.24-0.99). Countries with <4 data points were not used for fitting because they resulted in unrealistic trajectories (e.g. large drainage in 1700, overshoot in 2020). The sigmoidal curve replicates the economic stages of drainage expansion: capacity building, primary then secondary investments, and ending with saturation [51,70]. To reconstruct drainage time-series in data-poor countries (0<n<4), we transferred the midpoint and growth rate parameters, but not the upper asymptote, from data-rich exemplary countries within the same continent (Figure S15). This regionalization of the sigmoidal model allowed for the rate of growth and timing of the inflection point to be generalized across countries, while refitting the upper asymptote to the available data in each new country. To remain conservative, we set the highest reported data point as the upper asymptote of the sigmoidal curve. This upper limit ensures the cumulative mapped losses are constrained by available data. Uncertainty was not propagated from the fitted time series because of the large number of data-sparse countries for which uncertainty is difficult to meaningfully quantify. In the future, with additional metadata compiled from different data sources, a full assessment of the overlap, complementarity and agreement of data sources might be used to account for uncertainty in the national drainage statistics more systematically.

Annual peat extraction rates (tonnes $year^{-1}$; Figure S16) were interpolated linearly between data points. We also extrapolated extraction rates back in time assuming a doubling of extraction rates every decade prior to our first data point to replicate the rapid growth observed in data rich countries (e.g., Russia, USA). The continuous interpolated and extrapolated extraction rates were then used to calculate the cumulative tonnage of dry peat extracted per country since 1700 (Figure S17). The cumulative peat mass extracted was converted to an area of peatland drained using a conversion rate of 300,000 tonnes of dry peat per $km^2$ [71]. Sigmoidal curves were fitted to the cumulative area of peatland extracted to extend the time series to 2020. Then, sigmoid parameters were generalized to countries with only data on extracted peatland area but not extracted peat mass following the generalization approach described above.

Data on the area of wetland cultivation were found only for the period after 1980, preventing us from fitting sigmoidal functions. Instead, we assumed that wetland cultivation has occupied a constant country-specific fraction of cropland area over time. To estimate the area of wetland cultivation over the 1700-2020 period, we calculated the fraction of cropland reported as wetland cultivation per country during 2000-2020, when most data existed, and multiplied it with the cropland area taken from historical land use maps (see below). Given the long history of hydrological manipulation and cultivation of several wetland crops (e.g., rice, yam), going back to the Neolithic period [72–74], this assumption likely produces conservative estimates of wetland cultivation in 1700 and earlier. Despite its limitations, this assumption is preferable to its

alternative, namely to consider that the area of wetland cultivation in 2000-2020 has remained static through time which would result in a wetland cultivated area in 1700 that is three times higher than that derived from our fractional assumption.

For each of the four land use drivers above, country-level reconstructed time series were disaggregated to subnational units in 18 countries where subnational data were available (Figure S4). Because subnational data were generally not available to fit subnational sigmoid functions over sufficiently long periods (Figure S18), we calculated the fraction of each subunit within the national totals for the median year of subnational data. We then used these static fractions to distribute drainage over 1700-2020 to subnational units where drainage was prevalent in more recent years. This approach, however, could not capture changes in the subnational distribution of drainage within the same country over time.

*Generating a potential wetland cover:* To help allocate wetland loss, we generated potential wetland maps that represent the areas where wetlands may have formerly existed but are not occupied by present-day wetlands. We computed the potential wetland area as the difference between simulated and present-day wetland. Simulated wetland cover is greater than present-day cover in nearly all grid cells, but the subtraction can yield some sparsely distributed negative grid cells. Negative values of potential wetland area were set to zero and interpreted as areas where wetlands are underestimated by simulations. We generated 12 potential wetland maps from the cross-combinations of 4 simulated wetland maps and 3 present wetland maps (Figure S19). Together, the ensemble of 12 potential wetland maps is used to quantify the uncertainty from past and present wetland cover on the estimates of loss.

*Mapping drainage from national records:* We distributed drained (i.e., lost or converted) area ($km^2$) from national data ($L_{data}$) within the borders of each country over a 0.5° grid proportionally to the co-occurrence between potential wetland and land use area. The co-occurence, or overlap of land use and potential wetland approximates the geographic distribution of land use exposed to wet conditions. Because sub-grid cell overlap within the 0.5° grid cells can neither be resolved nor varied across time periods and regions, the overlap assumes random distribution between potential wetland and land use (i.e., multiplied grid cell fractions). The grid cell fractions were calculated based on land areas excluding lakes, rivers, ocean, and steep slopes where neither land use nor wetlands are likely to occur [65]. Grid cells where either no wetland area or no land use existed received no drainage. In the special case of peatland extraction, we prioritized extraction in peatlands near population centers by distributing peat extraction proportionally to $\log_{10}$ of population. Each of the four land use extents that represent a part of the nationally reported wetland drainage $L_{data}$ (Eq.1) were mapped individually based on the co-occurence of their respective land use and potential wetland.

$$L_{data} = L_{cropland} + L_{forestry} + L_{peat.extr.} + L_{wet.cultiv.} \quad (1)$$

*Modeling losses from other land uses:* We estimated the wetland area lost to the three land uses without drainage data (i.e., irrigated rice, pasture, and urban areas), but with available land use maps, by optimizing three parameters $\theta_i$, one per respective land use $i$. The calibrated parameters $\theta_i$ represent the tendency of each land use to replace natural wetlands, and are weighted in Eq. 2 by the joint probability $F_i$ of land use and potential wetland fractions $F_{wet.pot}$. For example, values of $\theta_i$ above1 represent a tendency to preferentially claim land for land use $i$ from wetlands as opposed to uplands. Each parameter $\theta_i$ is global, meaning it applies to all regions and time periods. For example, following Eq. 2, wetland area lost to irrigated rice is calculated as the product of $\theta_{rice}$ , the fraction of the grid cell occupied by rice ($F_{rice}$), the fraction of potential wetland ($F_{wet.pot}$) and the grid cell's total land area ($A$). Total wetland loss ($L_{total}$) in a grid cell is calculated as the sum of loss from the four land uses based on national data ($L_{data}$) and the loss from irrigated rice, pasture, and urban areas (Eq. 2). The three parameters $\theta_i$ are fitted through a comparison of the reconstruction with regional loss data (see paragraph below '*Calibrating reconstruction to regional data'*).

$$L_{total} = L_{data} + \left( \theta_{rice} F_{rice} + \theta_{pasture} F_{pasture} + \theta_{urban} F_{urban} \right) F_{wet.pot} A \quad (2)$$

*Mapping continuous drainage expansion:* At each decadal time step, wetland conversion from the seven land uses was distributed sequentially with the following priority order (first to last): wetland cultivation, irrigated rice, cropland, urban area, pasture, peat extraction, forestry. This order conceptually captures a succession of land use starting with conversions to artificial wetlands, followed by drainage for land uses of high importance, and finally drainage for land uses with lower economic returns. The ordering of drivers has a minor impact on overall results, and primarily affects the distribution of wetland loss within countries.

At each time step, newly added drained area is distributed across the land uses, then the undrained remainder of the land use is updated for the following time step to ensure that land area can only be drained once. The drained area in each grid cell is constrained by the total land use area in the grid cell. Conversely, the potential wetland area is not used as a fixed maximum drainage in a grid cell due to the uncertainty of simulated wetland cover. In some regions, the drained area can exceed the potential wetland extent. These upper-limits on the distribution of drained areas have caused minor divergences between the total area mapped and the original national statistics (Table S4).

*Estimating past wetland area:* The natural wetland area ($W$) at time $T$ is calculated by adding the cumulative loss ($L$) since time $t$ (in decremental order) to the wetland extent in 2020 ($W_{2020}$), following Eq. 3.

$$W_T = W_{2020} + \sum_{t=2020}^{T} L_t \quad (3)$$

*Estimating fractional wetland loss:*This approach estimates wetland area by sequential back-ward addition of the wetland loss, starting from the present-day reference, and thus ensures that the reconstruction aligns with present-day wetland maps. The justification for this approach is that present-day wetland maps are more reliable in their depiction of wetland areas than are simulated wetland maps. Hence, we used present-day wetland as the primary source of information for modeling the remaining wetland areas over time, while simulated wetland maps have a secondary effect on total losses (Figure S20) by affecting the area converted to the three modeled land uses (irrigated rice, pasture, and urban areas). The fraction of wetland lost since time $T$ is calculated by dividing the losses since time $T$ by the total wetland area $W_T$ at time $T$ (Eq. 4).

$$P_T = \sum_{t=2020}^{T} L_t / W_T \quad (4)$$

*Calibrating reconstruction to regional data:* We fitted the parameters $\theta_i$ to minimize the residuals of wetland fraction lost between our reconstruction and 121 regional wetland loss records. For each of the 12 potential wetland maps, we ran 5000 simulations with varying parameters $\theta_i$ that were generated using latin hypercube sampling. Values for $\theta_i$ were bound between $10^{-3}$ and 30 based on iteratively narrowing the range containing optimal parameters. Residuals of fraction wetland loss were weighted by region area, to ensure the reconstruction reproduced the major regions of loss. Simulations of parameters $\theta_i$ did not all reliably converge to an optimal set of three values. Therefore, we estimated the average and range of parameter values from the 100 best simulations per potential wetland map. The optimization equifinality is likely caused by internal model constraints and thresholds (e.g., drained area limited by land availability) that are insensitive to the values of parameters $\theta_i$.

The averaged best $\theta_i$ parameter ranges (Figure S21) across the 12 simulations were: $\theta_{rice}$ = 9.07 - 12.9, $\theta_{pasture}$= 11.3 - 15.6, $\theta_{urban}$= 0.19 - 1.23. The wide range of $\theta_{pasture}$ is caused by an added constraint limiting pasture drainage from exceeding the percentage of cropland drained in the same country and time period. This constraint is based on the understanding that economic investment toward drainage is generally first expended on cultivated land because pastures can be exploited for livestock grazing in wet conditions. We introduced this constraint to prevent pasture drainage from growing to an unreasonably large area and from compensating for gaps in drainage data. This constraint is the reason why the best reconstruction members

tend to be on the high end of the parameter range, as $\theta_{pasture}$ values beyond the pasture-cropland constraint have ceased influencing the mapped pasture drainage. The high fitted $\theta_{rice}$ value suggests that natural wetlands were preferentially used to claim land for irrigated rice culture and reflect the large extensive rice cultivation of China in the 20$^{th}$ century where nearly a third of regional data originates. This reliance on recent regional data may exaggerate conversion to rice in the decades after 1700. While we treat irrigated rice as a land use alongside others, other scenarios could be tested in the future, such as assuming all wet rice is first located in wetland areas and starts to expand upland only once wetland areas are exhausted. Wetland losses to urban areas are comparatively low, which can be explained by our inclusion of only direct wetland conversion (i.e., wetland to urban), whereas many urban areas may be located in former wetlands that were first converted to cropland.

The parameters $\theta_i$ varied only moderately among the 12 potential wetland simulations. Some potential wetland maps generated better agreement with regional wetland loss data. In particular, WAD2M was present in the top four scenarios. Among simulated wetland maps, the LPJ-wsl map led to higher regional agreement because its wetland coverage was more widespread which allowed it to distribute loss in areas where other maps estimated no wetland area. As a result, the reconstruction with highest agreement using the WAD2M present-day wetland map and LPJ-wsl simulated wetland is shown in Figures 1, 2 and 3 (and see Figure S22 for country timelines).

***Uncertainty assessment and validation***

We quantified the uncertainty of global wetland losses originating from three primary sources: 1) parameters $\theta_i$, 2) simulated wetland maps and 3) present-day wetland maps. To isolate the uncertainty from each of these three components, we computed the wetland losses from the 200 simulations with parameters $\theta_i$ achieving the highest agreement with regional data for each of the 12 potential wetland maps. The range of losses from this ensemble are shown in Figure 1A. Holding other factors constant, the range of wetland loss percentage from the best fit reconstructions is 0.7% across the the three different present-day wetland areas; is 1.7% from the four simulated wetland area; is 2.5% from their combination constituting the ensemble of twelve potential wetland cover; and is 3.9% from the $\theta_i$ parameter uncertainty (2.5$^{th}$ and 97.5$^{th}$ percentiles of parameters). This attribution underlines the uncertainty related to the modeled land uses (irrigated rice, pasture, and urban areas), greater than the contribution of the potential wetland to the overall uncertainty range of 7.1%. The range of uncertainty from the best fit reconstruction across the different present and simulated wetland maps, illustrates the importance of the fitting process in narrowing down this range. The fact that best-fit reconstructions are near the upper-bound of the uncertainty range also suggests that our reconstruction is likely conservative.

To evaluate the contribution of the three modeled land uses (irrigated rice, pasture, and urban areas), we compared wetland loss reconstructed from only the four land uses with national statistics to the regional data (i.e., $\theta_{rice}=\theta_{pasture}=\theta_{urban}=0$). With this reconstruction only from national statistics, we find moderate agreement ($R^2$ range=0.55-0.62 across ensemble of 12 reconstructions, n=121) and an overall underestimation of percentage loss (average bias: -18.0 to -25.5%; Figure S23). This bias indicates that the remaining disagreement is partially due to unaccounted drivers of wetland loss, and provides justification for their inclusion through modeling. Our ability to capture regional differences in drainage intensity of irrigated rice, pasture, and urban areas could be improved by applying a modeling scheme with varying parameters $\theta_i$ across regions and time periods. However, data availability does not currently allow for this.

Yet, even with the inclusion of the three modeled land uses, large disagreements in individual regions can arise from various causes. For instance, gaps in drainage data lead to underestimating wetland losses in some areas (e.g., Lake Chad), whereas losses in arid regions (e.g., Xinjiang in China) are underestimated because wetland simulations do not predict the former riverine wetlands, leading wetland drainage to be

distributed elsewhere. It is also possible that the independent literature estimates include additional drivers of loss that were not included in our reconstruction, possibly contributing to the negative bias in our results.

Finally, to evaluate the capacity of our calibrated model to generalize from a subset of the 121 regional estimates to new regions (i.e. providing a more representative accuracy over regions not covered by the regional data), we conducted a cross-validation exercise in which 90% of the data was used to fit the parameters $\theta_i$, and compared results to the 10% of withheld data for an independent accuracy estimate. The mapping and parameter fitting process was identical to the full reconstruction. Repeating this process across ten randomly sampled folds resulted in a training root mean squared error (RMSE) of 80.1 (range: 72.0-88.5; n=108) and validation RMSE of 82.0 (range: 55.5-110.4; n=12). This error gap suggests that the parameters $\theta_i$ generalize relatively well to new regions, but that the geographic clustering of regional loss data can lead to unstable results when large key regions are withheld from training. Conversely, small regions with high losses (e.g., Lake Urmia in Iran), that are difficult to capture by the coarse resolution of our approach, are adversely affecting model generalization to other regions.

***Regional summary of wetland loss***

We summarized the wetland area change across countries, river basins and petland regions. Hotspots of loss within and across countries were defined as contiguous areas with >50% wetland loss since 1700. We summarized losses by river basins with the basin outlines from the ISLSCP river network [75]. Peatland-rich regions were delineated by applying a 20% area threshold to the PEATMAP product [76], gridded at a 0.5° resolution. Global and regional peatland losses were estimated by assuming that the share of peatland *vs* other wetland loss is in proportion to their present share of coverage in each grid cell. This approach leads us to estimate that peatlands account for 15% of the losses from all seven land uses. However, this percentage is likely an underestimate because areas where peatlands were extirpated are overlooked (see Figure S7 for peatland distribution).

***Usage Notes***

Drainage and wetland extent were mapped at coarse resolution which may be inaccurate over small regions and short time periods. Use of our reconstructed maps should thus be reserved for applications at the continental to global scales. Available regional maps of drainage and wetland distribution which we could not integrate into our globally applicable method should be presumed more reliable locally and preferred for regional-scale studies.

**Acknowledgements**

Funding for this work was provided by a Postgraduate Scholarship from the Natural Sciences and Engineering Research Council of Canada, the David and Lucille Packard Fellowship in Science and Engineering, and National Science Foundation Grant DEB-1115025, DAAD visit to Bonn Universität, and by the Gordon and Betty Moore Foundation through Grant GBMF5439 “Advancing Understanding of the Global Methane Cycle” to Stanford University supporting the Methane Budget activity for the Global Carbon Project. B.D.S was funded by the Swiss National Science Foundation grant no. PCEFP2_181115.

**Author Contributions**

EF conceived and designed the study with input from JM, BDS, AM, ZZ, BP, PBM and RBJ. EF, SS, TM compiled drainage data. Wetland area data were provided by ZZ, BDS, JM and BL. Land use data was provided by KKG. EF developed the model calibration with advice from BDS, JM and ZZ. EF wrote the manuscript with input from PBM, and all authors edited the final version.

**Data availability**

Data will be submitted to a public data repository Zenodo simultaneously with publication. Temporary links are available for the review process:

Data 1: National and subnational statistics of drained or converted areas (.xlsx).

Data 2: Regional wetland percentage loss estimates and geospatial polygons (.csv and .shp).

Data 3: Gridded reconstruction of drained area per land use and cumulative, as well as natural wetland area (NetCDF).

**Methods references**


44. de Zeeuw, J. W. Peat and the Dutch Golden Age. The historical meaning of energy-attainability. *A A G Bijdr.* **21**, 3–31 (1978).

45. Woodward, C., Shulmeister, J., Larsen, J., Jacobsen, G. E. & Zawadzki, A. The hydrological legacy of deforestation on global wetlands. *Science* (2014) doi:10.1126/science.1260510.

46. Feick S., Siebert S., Döll P. *A Digital Global Map of Artificially Drained Agricultural Areas*. (2005).

47. *Irrigation and Drainage in the World – A Global Review (Vol. I, II, III).* (International Commission on Irrigation & Drainage, 1982).

48. FAO, 2019. FAOSTAT. Food and Agriculture Organization of the United Nations, Rome, Italy.

49. McCorvie, M. R. & Lant, C. L. Drainage District Formation and the Loss of Midwestern Wetlands, 1850-1930. *Agric. Hist.* **67**, 13–39 (1993).

50. Kearns, K. C. Development of the Irish Peat Fuel Industry. *Am. J. Econ. Sociol.* **37**, 179–193 (1978).

51. Schultz, B., Zimmer, D. & Vlotman, W. F. Drainage under increasing and changing requirements. *Irrig. Drain. Syst.* **56**, S3–S22 (2007).

52. Niu, Z. *et al.* Mapping wetland changes in China between 1978 and 2008. *Chinese Science Bulletin* vol. 57 2813–2823 (2012).

53. Dahl, T. E. *Wetlands Losses in the United States 1780's to 1980's: Report to Congress*. (1990).

54. Zhang, Z., Fluet-Chouinard, E. & Jensen, K. Development of the global dataset of Wetland Area and Dynamics for Methane Modeling (WAD2M). *Earth Syst. Monit.* (2021).

55. Prigent, C., Jimenez, C. & Bousquet, P. Satellite-Derived Global Surface Water Extent and Dynamics Over the Last 25 Years (GIEMS-2). *Journal of Geophysical Research: Atmospheres* vol. 125 (2020).

56. Lehner, B. & Döll, P. Development and validation of a global database of lakes, reservoirs and wetlands. *Journal of Hydrology* vol. 296 1–22 (2004).

57. Pekel, J.-F., Cottam, A., Gorelick, N. & Belward, A. S. High-resolution mapping of global surface water and its long-term changes. *Nature* **540**, 418–422 (2016).

58. Carroll, M. L., Townshend, J. R., DiMiceli, C. M., Noojipady, P. & Sohlberg, R. A. A new global raster water mask at 250 m resolution. *International Journal of Digital Earth* **2**, 291–308 (2009).

59. Portmann, F. T., Siebert, S. & Döll, P. MIRCA2000-Global monthly irrigated and rainfed crop areas around the year 2000: A new high-resolution data set for agricultural and hydrological modeling. *Global Biogeochem. Cycles* **24**, (2010).

60. Hugelius, G. *et al.* The Northern Circumpolar Soil Carbon Database: spatially distributed datasets of soil coverage and soil carbon storage in the northern permafrost regions. *Earth System Science Data* **5**, 3–13 (2013).

61. Gumbricht, T. *et al.* An expert system model for mapping tropical wetlands and peatlands reveals South America as the largest contributor. *Glob. Chang. Biol.* **23**, 3581–3599 (2017).

62. Zhang, Z., Zimmermann, N. E., Kaplan, J. O. & Poulter, B. Modeling spatiotemporal dynamics of global wetlands: comprehensive evaluation of a new sub-grid TOPMODEL parameterization and uncertainties. *Biogeosciences* **13**, 1387–1408 (2016).

63. Beven, K. J. & Kirkby, M. J. A physically based, variable contributing area model of basin hydrology / Un modèle à base physique de zone d'appel variable de l'hydrologie du bassin versant. *Hydrol. Sci. Bull.* **24**, 43–69 (1979).

64. Wania, R. *et al.* Present state of global wetland extent and wetland methane modelling: methodology of a model inter-comparison project (WETCHIMP). *Geosci. Model Dev.* **6**, 617–641 (2013).

65 Goldewijk, K. K., Beusen, A., Doelman, J. & Stehfest, E. Anthropogenic land use estimates for the Holocene – HYDE 3.2. *Earth System Science Data* vol. 9 927–953 (2017).

66. Goldewijk, K. K., Beusen, A., Van Drecht, G. & De Vos, M. The HYDE 3.1 spatially explicit database of human-induced global land-use change over the past 12,000 years. *Global Ecology and Biogeography* vol. 20 73–86 (2011).

67. Hurtt, G. C. *et al.* Harmonization of global land use change and management for the period 850–2100 (LUH2) for CMIP6. *Geoscientific Model Development* vol. 13 5425–5464 (2020).

68. Xu, J., Morris, P. J., Liu, J. & Holden, J. PEATMAP: Refining estimates of global peatland distribution based on a meta-analysis. *CATENA* vol. 160 134–140 (2018).

69. Matheson, D. P. A. *nls.multstart: Robust Non-Linear Regression using AIC Scores*. (2020).

70. Smedema, L. K., Abdel-Dayem, S. & Ochs, W. J. Drainage and Agricultural Development. *Irrig. Drain. Syst.* **14**, 223–235 (2000).

71. Murphy, F., Devlin, G. & McDonnell, K. Benchmarking Environmental Impacts of Peat Use for Electricity Generation in Ireland—A Life Cycle Assessment. *Sustain. Sci. Pract. Policy* **7**, 6376–6393 (2015).

72. Denham, T. Archaeological Evidence for Mid-Holocene Agriculture in the Interior of Papua New Guinea: A Critical Review. *Archaeology in Oceania* **38**, 159–176 (2003).

73. Fuller, D. Q. & Qin, L. Water management and labour in the origins and dispersal of Asian rice. *World Archaeol.* **41**, 88–111 (2009).

74. Bellwood, P. The Checkered Prehistory of Rice Movement Southwards as a Domesticated Cereal—from the Yangzi to the Equator. *Rice* **4**, 93–103 (2011).

75. Vörösmarty, C. J. & Fekete, B. ISLSCP II River Routing Data (STN-30p). *ISLSCP Initiative II Collection*, (2011) doi:10.3334/ORNLDAAC/1005.

76. Xu, J., Morris, P. J., Liu, J. & Holden, J. PEATMAP: Refining estimates of global peatland distribution based on a meta-analysis. *Catena* **160**, 134–140 (2018).